REPORT DOCUMENTATION PAGE

AFRL-SR-AR-TR-05-

0516

Management and Budget, Paperwork Reduction Project (0704-0188), Washington, DC 20503

1. AGENCY USE ONLY (Leave blank)	2. REPORT DATE	3. REPORT TYPE AND DATES
	18 October 2005	Final 05/01/2001 to 10/31/2004

4. TITLE AND SUBTITLE
Studies of Heterogeneous and Diffusion-Influenced Nucleation for Improved Processing of Nanostructural Materials

5. FUNDING NUMBERS
F49620-01-1-0355

6. AUTHOR(S)
Dr. Kenneth F. Kelton
Dr. William E. Buhro

7. PERFORMING ORGANIZATION NAME(S) AND ADDRESS(ES)
Washington University
Campus Box 1054
One Brookings Drive
St. Louis, MO 63130

8. PERFORMING ORGANIZATION REPORT NUMBER

9. SPONSORING / MONITORING AGENCY NAME(S) AND ADDRESS(ES)
AFOSR/PK4
USAF, AFRL
AF Office of Scientific Research
801 N. Randolph St., Room 732
Arlington, VA 22203-1977

NA

10. SPONSORING / MONITORING AGENCY REPORT NUMBER

11. SUPPLEMENTARY NOTES

12a. DISTRIBUTION / AVAILABILITY STATEMENT

Approved for public release,
distribution unlimited

12b. DISTRIBUTION CODE

13. ABSTRACT ***(Maximum 200 Words)***

The high strength to weight ratio of amorphous and nano-structured Al-based alloys make them particularly interesting for aerospace applications. The purpose of this grant was to identify a suitable glass for studies of the nucleation processes leading to nano-structure formation and to investigate the possibility of using TiB_2 for enhanced microstructure refinement during crystallization.

The goals of the grant were met and exceeded. We (i) identified $Al_{88}Y_7Fe_5$ as a model glass for study; (ii) discovered that microalloying significantly improved glass formation and stability with the substitutions of small amounts (≈0.5 at.%) of Ti, Zr and V for the Al; (iii) discovered amorphous $Al_{85.35}Y_7Fe_5Ti_{0.5}$ by the addition of TiB_2 particles, producing a final grain density of approximately $10^{24}/m^3$ on the surfaces of the particles. In addition to demonstrating the technological usefulness of microalloying and the indication that evenly dispersed nanoparticles of TiB_2 should lead to a significant nano-structure refinement during crystallization, these results also raise new fundamental questions, such as the mechanism of microalloying.

14. SUBJECT TERMS			15. NUMBER OF PAGES
			16. PRICE CODE
17. SECURITY CLASSIFICATION OF REPORT	18. SECURITY CLASSIFICATION OF THIS PAGE	19. SECURITY CLASSIFICATION OF ABSTRACT	20. LIMITATION OF ABSTRACT

NSN 7540-01-280-5500

Standard Form 298 (Rev. 2-89)
Prescribed by ANSI Std. Z39-18
298-102

Final Technical Report

Studies of Heterogeneous and Diffusion-Influenced Nucleation for Improved Processing of Nanostructural Materials

Contract
AFOSR - F49620-01-1-0355

Prepared for
AIR FORCE OFFICE OF SCIENTIFIC RESEARCH

For the Period
05/01/01-10/31/04

Submitted by:

Kenneth F. Kelton, Principle Investigator
William E. Buhro, Co-Principle Investigator

Departments of Physics and Chemistry
Washington University, St. Louis, Missouri 63130

Table of Contents

Abstract

The high strength to weight ratio of amorphous and nano-structured Al-based alloys make them particularly interesting for aerospace applications. The purpose of this grant was to identify a suitable glass for studies of the nucleation processes leading to nano-structure formation and to investigate the possibility of using TiB_2 for enhanced microstructure refinement during crystallization.

The goals of the grant were met and exceeded. We (i) identified Al_{88},Y_7Fe_5 as a model glass for study; (ii) discovered that microalloying significantly improved glass formation and stability with the substitutions of small amounts ($\approx$ 0.5 at.%) of Ti, Zr and V for the Al; (iii) discovered amorphous $Al_{85.35}Y_8Fe_6V_{0.65}$ with the largest supercooled region known in an Al-based glass; and (iv) demonstrated the catalyzed nucleation of the α-Al phase in $Al_{87.5}Y_7Fe_5Ti_{0.5}$ by the addition of TiB_2 particles, producing a final grain density of approximately $10^{24}/m^3$ on the surfaces of the particles. In addition to demonstrating the technological usefulness of microalloying and the indication that evenly dispersed nanoparticles of TiB_2 should lead to a significant nano-structure refinement during crystallization, these results also raise new fundamental questions, such as the mechanism of microalloying.

List of Figures

List of Tables

Executive Summary

Light-weight aluminum-based glasses are of significant interest because of their high strength-to-weight ratios and other favorable mechanical properties, which give them potential for aerospace applications. Partially crystallized nanocomposites produced from these glasses have even greater technological potential, because their tensile strengths, hardness, stiffness, and ductilities significantly surpass those of the glasses. At present, all Al-based glasses are obtained by rapid quenching from the melt, which severely limits the availability and applications potential of the partially crystallized nanocomposites derived from them. Furthermore, the mechanisms for nanostructure development in the nanocomposites during thermal processing are unknown, precluding systematic control and optimization of their mechanical behavior. Therefore, the primary goals of this research were to enhance the stabilities of aluminum-transition-metal-rare-earth (Al-TM-RE) glasses, and to elucidate the nucleation-and-growth mechanisms active during their partial crystallization upon thermal processing.

The specific motivations were as follows.

- To identify optimal compositions for Al-based glasses for basic investigations and for potential applications,
- To develop a new, coupled-flux nucleation model to probe the mechanisms of nanocrystallization in the glasses,
- To determine if controlled nanocrystallization could be induced by heterogeneous nucleation.

The key findings of this work were as follows.

- Small microadditions of Ti, Zr, or V to Al-Y-Fe alloys dramatically enhanced glass stability and formability.
- A vanadium microalloy of type Al-Y-Fe-V was discovered that exhibits the highest thermal stability and largest supercooled region of any known Al-based glass. The thermal properties of this amorphous alloy suggest that the critical-cooling rate for glass formation may be reduced by two orders of magnitude. This discovery further suggests that Al-rich bulk glasses having similar compositions might be accessible by conventional melt cooling.
- An increased nucleation rate on *heterogenous* TiB_2 nucleants incorporated into the glasses indicated their potential for further nanostructure control and refinement, even in glasses with very high *homogenenous* nucleation rates.

The questions for further study included the following.

- What is the mechanism by which small concentrations of Ti, Zr, and V alter glass crystallization?
- Can further stoichiometric and microaddition modifications produce Al-rich glasses at conventional, slow cooling rates in the range of 1 – 20 K/s?
- Can detailed structural studies of glasses prepared with different composition and under different processing conditions provide insight into the role of this microalloying?

I. Introduction and Motivation

The discoveries of light-weight aluminum-based glasses and new families of metallic glasses that form at cooling rates more typical of silicate glasses have led to a renaissance in the study of metallic glasses. Inoue *et al.* [1,2] and He *et al.* [3] first reported glass formation in alloys containing greater than 80 at. % Al. These glasses are of significant interest because of their high strength-to-weight ratios and other favorable mechanical properties (see [4] for a recent review).

Amorphous/nanocrystal composites (nano-composites) resulting from the partial crystallization (devitrification) of Al-transition metal-rare earth (Al-TM-RE) glasses are even more interesting and have even greater technological potential, because their mechanical properties significantly surpass those of the glasses [4,5]. Figure 1 compares the tensile strengths of conventional, coarse-grained Al alloys (a and b) to those of Al-RE-TM glasses (c) and partially devitrified nanocomposites (d) [5]. Notably, the tensile strengths of the partially devitrified nanocomposites achieve values in the range of 1200-1500 MPa, substantially higher than those achieved by conventional Al alloys or Al-RE-TM glasses. The microstructures of the Al-RE-TM nano-composites consist of 5-20 nm α-Al nanocrystals finely dispersed in an amorphous alloy matrix at typical levels of 20-25 volume % [4].

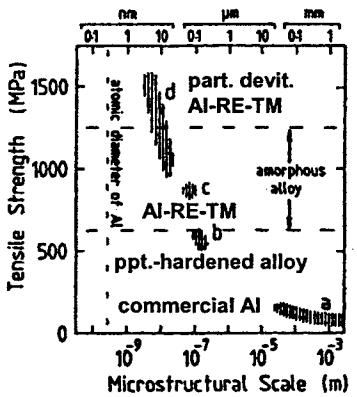

Figure 1 – Relationship between grain size and room-temperature tensile strength for Al-based alloys [5]. Conventional Al alloys (a and b), Al-RE-TM glasses (c), and partially devitrified Al-RE-TM nanocomposites (d) are compared.

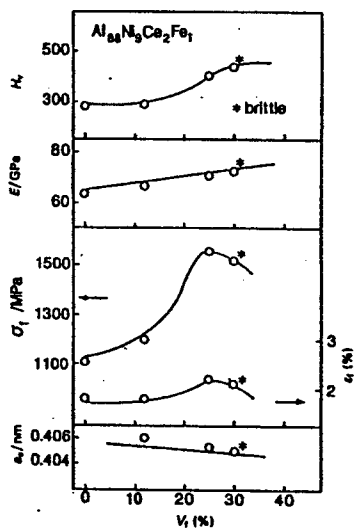

Figure 2 – Dependence of hardness (H_v), Young's modulus (E), tensile fracture strength (σ_f), fracture elongation (ε_f), and lattice parameter (a_0) on α-Al nanocrystal volume fraction in $Al_{88}Ni_9Ce_2Fe_1$ [4].

Figure 2 shows the dependence of mechanical properties on the nanocrystal volume fraction in a representative Al-RE-TM nano-composite [4]. Hardness, Young's modulus, tensile fracture strength, and fracture elongation all exhibit significant increases at a

nanocrystal volume fraction of about 20%. The enhanced mechanical properties in the Al-RE-TM nano-composites are thought to be due to the high solute content in the amorphous matrix [6], and interaction between the dispersed Al nanocrystals and shear bands that develop upon deformation of the amorphous matrix[4]. The dispersed α-Al nanocrystals also provide significant ductility.

Several questions motivated the research performed under AFOSR contract F49620-01-1-0355:

- Not all glasses crystallize to nano-structured composites. There is a need to predict and identify optimal compositions for candidate glasses, and to establish the necessary processing control. The mechanisms for nanocrystallization are not well understood, hindering these goals.

- It is clear that since the solubility of rare earth atoms in Al is extremely small, the formation of α-Al during the crystallization of many Al-TM-RE glasses must require long-range diffusion in both the nucleation and the growth step. While the commonly used classical theory of nucleation cannot be used to quantitatively analyze this case, a new model developed by Kelton, which takes account of the coupling between the interfacial and long-range diffusion fluxes can. A suitable Al-TM-RE glass can, then, be used as a probe of that new model and lead to a better understanding of the nanocrystallization mechanisms.

- Can nanocrystallization be promoted by deliberately introducing heterogeneities? TiB_2 innoculants are commonly used as grain refining agents in conventional cast Al, but it is questionable whether this would be effective in cases where the nucleation rates already approach $10^{19}/m^3s - 10^{20}/m^3s$, as is the case in many Al-based metallic glasses.

- Some presumed Al-RE-TM glasses do not show peaks in the curves obtained from isothermal DSC (Differential Scanning Calorimetry) experiments. This has been argued to indicate either a high density of quenched in nuclei, or grain coarsening, implying that they are not true glasses. It is important to determine which is the correct interpretation, since it will impact the parameter space chosen for true glass formation.

The research conducted under AFOSR contract F49620-01-1-0355 successfully addressed several of these questions. The key findings were:

- Rapidly-quenched alloys of $Al_{88}Y_7Fe_5$, widely viewed as glasses, do not show a peak in their DSC isothermal curves nor a discernable glass transition temperature, raising the concern that these may actually be amorphous/nanocrystal composites.

- Microalloying exerts a great influence on the glass formability and crystallization behavior of Al-RE-TM alloys. The addition of as little as 0.5 at.% of Ti, Zr, and V to the $Al_{88}Y_7Fe_5$ alloys produced materials with clear glass transition temperatures,

peaks in the DSC isothermal curves and an increased transformation temperature to α-Al.

- The addition of 0.65 at.% of V in an Al-Y-Fe alloy produces a metallic glass with the largest supercooled region of any Al-based glass, suggesting the existence of Al-rich compositions that could form glasses at slow (conventional) cooling rates.

- An enhanced nucleation rate on the surfaces of micrometer sized grains of TiB_2 in AlYFeTi glasses, suggesting that if a method were found to disperse nanocrystals of TiB_2, they would effectively catalyze nucleation, even in glasses with an enormous homogeneous nucleation rate.

These findings enhance our understanding of nanocrystallization in the Al-based glasses and offer potential routes for improved nanostructure control.

II. Background

Before presenting and discussing the key results from the research sponsored by AFOSR contract F49620-01-1-0355, it is useful to present some background material.

Nucleation mechanism for nanocrystallization

The reasons for the development of uniform nanoscale devitrification microstructures in many of the recently discovered Zr-based, Al-based, Fe-based, and Mg-based metallic glasses remain largely unknown. The nanostructures observed, with grain densities ranging from $10^{20}/m^3$ - $10^{23}/m^3$, and corresponding grain diameters between 5 and 20 nm, signal extremely high nucleation rates and low growth velocities [8, 9]. Typically, the grain-growth rate is rapid for small grains, but slows abruptly when the grain diameter exceeds a few nm [10]. Further, the nucleation rate is strongly time-dependent, increasing during the early stages of crystallization but decreasing dramatically with longer anneals[11]. In some Zr-based metallic glasses that form quasicrystals, the high nucleation rate may be due, in part at least, to icosahedral short-range order in the glass[12-14]. Nanostructure formation in devitrified glasses is more common than this, however, and is found also in glasses that do not form the icosahedral phase. Suggested reasons include quenched-in nuclei [15], heterogeneous precipitate formation[16], phase separation [17] and the influence of composition[18, 19], and diffusion-controlled nucleation [9].

Beginning in the 1950s, primarily due to electron-microscopy studies, it became obvious that phase separation occurred in many glass-forming systems (at that time, silicate glasses)[20-23]. Phase separation has also recently been identified in amorphous metals, based on evidence from small-angle x-ray scattering [24-26], atom-probe studies [27-30], and energy-filtered TEM studies[11]. Phase separation plays an important role in glass stability and devitrification and has been increasingly exploited for developing new glasses[31]. Many glasses, however, show no evidence for phase separation, making it unlikely to be the sole source of nanostructure formation upon crystallization.

The high nucleation density is unlikely to occur by normal heterogeneous nucleation. This would require that the sample contain 10^{20}-10^{23} nucleants per m^3, exceeding that normally found by 5-10 orders of magnitude. But, if the glass were supersaturated in an element that if precipitated could serve as a heterogeneous site, it might be possible to attain this density. This is believed to occur when small amounts of Cu are added to the well-studied FeBSi glasses [27, 32]. Primary crystallization in these doped glasses produced a microstructure consisting of 10 nm diameter grains of the bcc α-Fe(Si) phase embedded in the glass. Like phase separation, however, this mechanism is unable to explain the general tendency for nanostructure formation.

Growth on quenched-in nuclei has been offered as an explanation for the high grain density [33 , 34]. However, while quenched-in nuclei are always present in glasses, the nuclei density is less than expected from steady-state considerations because transient nucleation suppresses the rate during the quench[35], making it even more difficult to

explain the extremely high nucleation rates required to produce the high density of nuclei observed.

A key feature of most glasses that form nanostructures is a different composition of the primary crystallizing phase from the glass, making long-range diffusion effects important for nucleation and growth. This is particularly true for the Al-transition metal-rare earth (Al-TM-RE) glasses, where the primary crystallization kinetics of α-Al are primarily determined by the slow diffusion of the RE atoms. The measured particle size distributions suggest time-dependent nucleation rates with saturation due to soft impingement resulting from the long-range diffusion fields that are established during the nucleation and growth in these glasses[11]. Further, the data appear to contain two peaks – suggesting that quenched-in nuclei might play an important role in devitrification. One explanation for the high nucleation rate is that it arises from a quenched-in distribution of small clusters that are surrounded by a glass that has a concentration closer to that of the crystal[9].

Microalloying

A strong dependence of glass formation and stability on small additions of various, generally reactive, elements, at levels of a few percent or less, is well known in Zr-based glasses [14]. Stabilization of Cu- [36] and Fe-based [37] glasses with microadditives is also known. However, to our knowledge similar "microalloying" effects in Al-based glasses were not reported prior to our work. Why such small concentrations of microadditives have such a profound influence over glass stability is unclear. The common interpretation is that the dopants act as oxygen scavengers [37-41]. A second interpretation suggests that the microadditions alter the local structure of the liquid or glass [14, 42]. As will be discussed, our data support this second viewpoint for the influence of Ti, Zr, and V microadditives to Al-rich glasses. We are currently conducting the detailed structural studies necessary to fully elucidate the mechanisms of stabilization.

III. Sample Preparation and Characterization

These studies focused entirely on Al-Y-Fe alloys. $Al_{88}Y_7Fe_5$ and $Al_{88-x}Y_7Fe_5Ti_x$ (with x = 0.5, 1, 2) ingots were prepared by arc-melting the elemental components on a water-cooled copper hearth, which was first evacuated to $3x10^{-2}$ Torr and backfilled with high-purity Ar gas (99.999%). A Ti-getter located close to the samples was melted prior to arc-melting to further remove oxygen from the chamber. The samples were flipped and re-melted several times to ensure a homogeneous composition; the duration of each melt cycle was approximately one minute. To investigate possible oxygen contamination, samples were re-melted either two times or four times. Amorphous ribbons were prepared by melting the ingots using rf-induction heating to 1100-1150°C (well above the liquidus temperature) in a graphite crucible under an Ar atmosphere, and rapidly quenching the liquid onto a copper wheel rotating at 3800 m/min. The quenched ribbons were continuous for 10-250 cm and had an average cross section of 1-2 mm by 20-30 μm. Samples were characterized by x-ray diffraction, a JEOL 2000FX TEM, equipped with a Noran energy-dispersive x-ray spectrometer (EDXS), and differential scanning calorimetry (DSC), using a Perkin-Elmer DSC7 that had a modified gas-handling system to minimize sample oxidation.

IV. Research Results and Discussion

A detailed discussion of each of these primary results follows.

A. Microalloying and the influence of oxygen

$Al_{88}Y_7Fe_5$, a widely studied Al-based rapidly-quenched alloy, shows glass-like x-ray and TEM diffraction patterns, no evidence for crystal diffraction peaks or precipitates in TEM bright-field images, and an exothermic peak in nonisothermal differential scanning calorimetry (DSC) measurements [43]. However, the nonisothermal DSC curves show no evidence for a glass transition and isothermal DSC studies show a monotonic decrease in the rate of heat evolved with annealing time (fig.3.*a*). This behavior is taken to be characteristic of grain coarsening[44], suggesting that the quenched alloys are actually partially nanocrystalline. It is also argued by some that the lack of the isothermal DSC peak could be evidence for quenched-in nuclei, but for normal transformations the growth on quenched-in nuclei would still produce a peak unless the sample were significantly crystallized (> 50-60% transformed).

Additions of small amounts of Ti dramatically improve glass-formation and stability. A glass-transition temperature becomes evident in nonisothermal DSC studies and the isothermal DSC curves show peaks that are characteristic of nucleation and growth during glass crystallization (fig. 3.a). Zr and V microadditions were found to also enhance glass formation in these alloys; surprisingly, Hf did not enhance glass formation or stability.

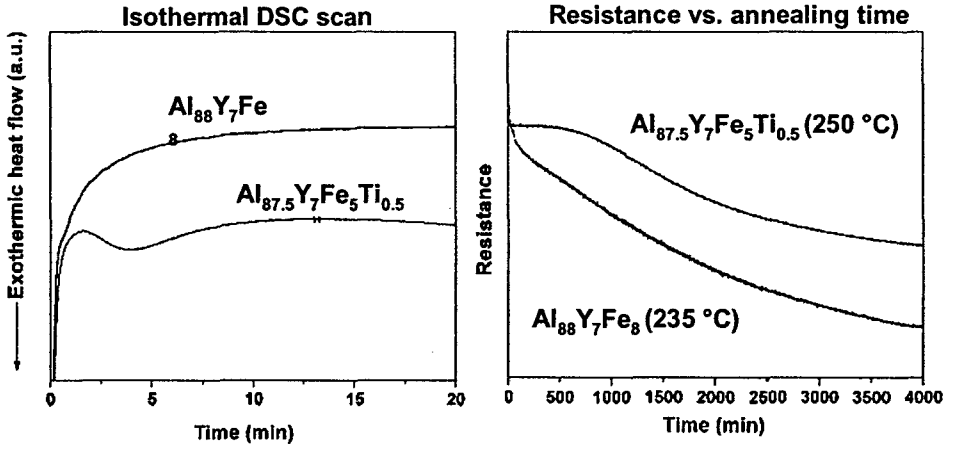

Figure 3 – ***(left)*** DSC isothermal trace of rapidly quenched $Al_{88}Y_7Fe_5$ and $Al_{87.5}Y_7Fe_5Ti_{0.5}$. (***right***) Change in resistance with isothermal annealing time for the same two alloys.

In-situ four-probe measurements of the changes in the resistance of rapidly quenched Al-RE-TM alloys were made using a computer-controlled dc bridge. A discussion of the furnace, sample holder and bridge circuit is given elsewhere [45]. The measured changes

in resistivity for $Al_{88}Y_7Fe_5$ and $Al_{87.5}Y_7Fe_5Ti_{0.5}$ are shown in fig. 3.b. The sigmoidal shape of $\Delta R(t)$ for $Al_{87.5}Y_7Fe_5Ti_{0.5}$ is consistent with a nucleation and growth mechanism; the monotonic change in $\Delta R(t)$ for the $Al_{88}Y_7Fe_5$ sample suggests coarsening. These data are then consistent with our isothermal DSC data, suggesting that the rapidly quenched $Al_{88}Y_7Fe_5$ alloy is a nanostructured material.

The glass-stabilization mechanism by the Ti microadditive is unclear. Our studies indicated that oxygen contamination during processing could significantly influence the phases that formed. If Ti (or Zr and V) were simply scavenging internal oxygen, however, the small quantity of Ti added should be consumed quickly if the oxygen concentration in the alloy were increased, giving ribbons more similar to those made without Ti. To check this, oxygen was deliberately introduced into the samples by adding Fe_2O_3. As shown in figure 4.a, the α-Al crystallization DSC peak did not change significantly with the addition of oxygen. The intensity of the second peak (the formation of a metastable phase, MP) decreased radically in the oxygenated samples; the third peak also decreased, but to a lesser extent. A new DSC peak appearing near 370 °C signaled the formation of a bcc phase (a = 0.317 nm). The addition of oxygen, then, destabilizes the metastable phase or phases that form near 340 °C. However, rapidly quenched samples made with >0.5 atomic % oxygen were not amorphous, irrespective of the amount of Ti present. The same results were obtained with O_2 addition to an Al-Y-Fe glass containing V instead of titanium.

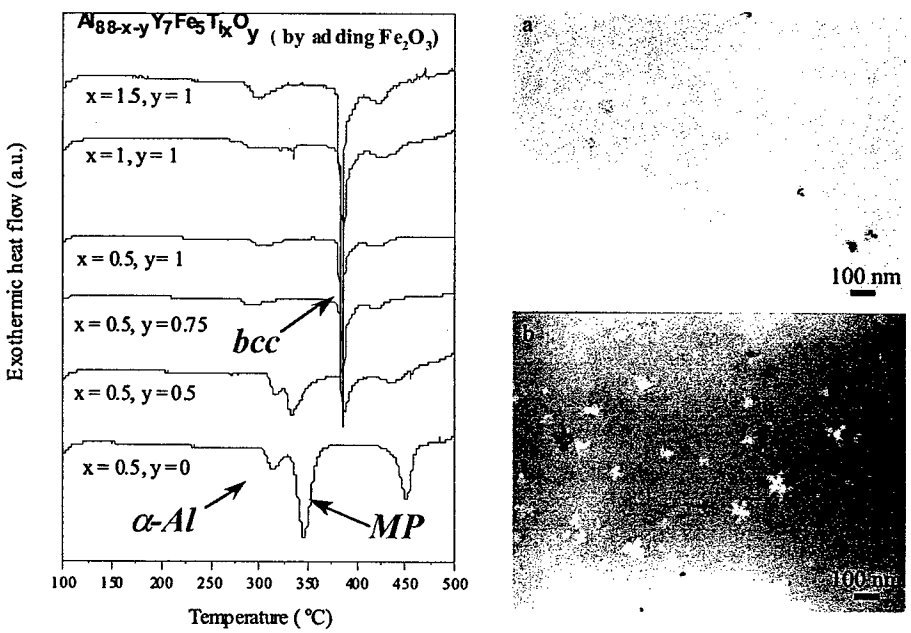

Figure 4 – ***(left)*** Nonisothermal DSC traces for AlYFeTi samples made with different concentrations of oxygen and Ti. $Al_{88}Y_7Fe_5$ annealed at 250 °C for 30 min (***top right***) and $Al_{87.5}Y_7Fe_5Ti_{0.5}$ annealed at 280 °C for 30 min (***bottom right***).

Transmission electron microscopy (TEM) images of annealed alloys show the stabilizing influence of small additions of Ti. For $Al_{88}Y_7Fe_5$, α-Al crystals appear after annealing at 250 °C for 30 min (fig. 4 *top right*). To produce a sizable density of α-Al crystals in $Al_{87.5}Y_7Fe_5Ti_{0.5}$ for the same time requires a higher annealing temperature (280 °C) but even then the crystal density is lower, reflecting a lower nucleation rate. The larger crystal size indicates that Ti primarily influences the nucleation barrier instead of the growth rate. The dendritic crystal shapes indicate that growth is diffusion limited in both alloys. It appears, then, that Ti raises the nucleation barrier for α-Al by altering the structure of the liquid/glass, either changing the driving free energy or, more likely, the crystal-glass interfacial free energy. This is supported by recent work, jointly supported by Kelton's NSF grant and our current AFOSR grant. High-q synchrotron x-ray diffraction studies, EXAFS studies made in collaboration with A. Sadoc (Paris) and fluctuation TEM studies made in collaboration with P. Voyles (U. Wisconsin) all indicate subtle structural differences between the rapidly quenched alloys made with and without Ti.

B. Crystal-size distributions

Figure 5 shows initial measurements made on rapidly quenched alloys that were annealed at 270°C for 60 minutes. Two peaks are evident in the histogram; the smaller peak at larger particle sizes corresponds to those crystals that grew first and may correspond to quenched-in nuclei. The second peak reflects subsequent nucleation, likely homogeneous from the high grain density (approximately $10^{21}/m^3$).

The high density of quenched-in nuclei inferred from the two peaks in fig. 5 is difficult to explain within the classical theory. During a rapid quench, the slowing of the kinetic processes underlying the evolution of the cluster distribution with decreasing temperature causes a deviation of the cluster population from that expected for steady state nucleation [48]. As a result, the nucleation rate during the quench can be orders of magnitude less than the steady state rate [49]. Were the crystal density observed after annealing (of order $10^{21} - 10^{23}/m^3$) to arise from nuclei produced during the quench, then, the steady-state nucleation rate would need to be unreasonably high.

Surprisingly, the solution to this problem may lie in taking proper account of long-range diffusion processes. A key feature of all glasses that form nano-structures is a different composition of the primary crystallizing phase from the glass, making long-range diffusion effects important for both nucleation and growth. This is particularly true for the Al-3d transition metal-rare earth (Al-TM-RE) glasses, where the primary crystallization kinetics of α-Al are primarily determined by the slow diffusion of the RE atoms. The classical theory of nucleation, however, cannot properly describe diffusion-controlled nucleation, since it is inherently an interface-limited theory.

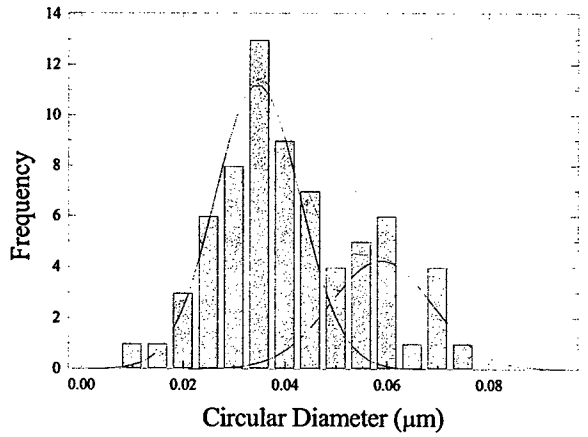

Figure 5 - Measured crystallite density for an $Al_{87.5}Y_7Fe_5Ti_{0.5}$ glass after annealing for 270 °C for 60 minutes.

To treat this problem, Kelton constructed a coupled-flux model that links the stochastic fluxes of interfacial attachment and long-range diffusion [50,51]. Following an approach first suggested by Russell [52], attention is focused on three regions: the cluster, the immediate neighborhood around the cluster (the shell region), and the parent phase (fig. 6). The nucleation kinetics are a function of both the number of atoms in the cluster, *n*,

and the number of atoms in the cluster neighborhood, ρ. Predictions from the coupled-flux model approach those from the classical theory in the limit of high concentration and high diffusion rates in the parent phase. Because clusters smaller than the critical size are on average dissolving, the coupling of the interfacial and diffusion fluxes increases the flux into the shell region, leading to a time-invariant concentration that is closer to that of the new phase than the parent phase, the opposite of what is expected for growth. If retained during the quench this will bias small clusters to grow much faster than the kinetics determined from measured diffusion-limited growth rates would predict, leading to a rapid increase in the population of small nuclei and explaining the apparently enormous nucleation rate. This model, then, offers a possible explanation of how quenched-in nuclei can be sufficiently effective, despite the radical decrease in their density with quenching. Further, the rapid cluster growth depletes the region near the clusters, causing an abrupt arrest in their growth rates and leading to the observed nano-structure. The magnitude of this effect will depend on the materials parameters and the quenching rate. Even if the quenched-in regions are insufficient to contribute significantly, the potentially large change in steady-state nucleation rates and induction times will have a profound impact on the crystallization kinetics.

In support of these arguments, a coupled-flux nucleation model has produced much better agreement between experimental and calculated diffusion-controlled oxygen precipitation rates in silicon [53]. The $Al_{87.5}Y_7Fe_5Ti_{0.5}$ glass developed under this grant is well suited for quantitative nucleation studies, allowing the coupled-flux argument for nano-structure formation to be more directly probed.

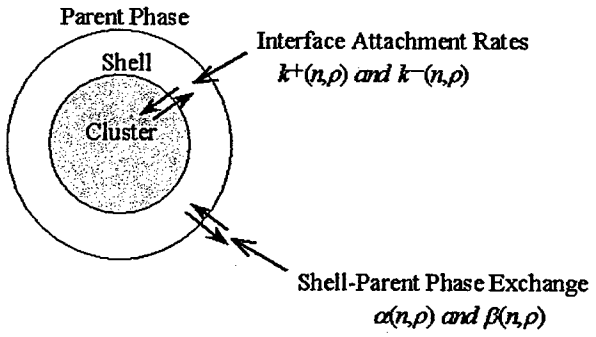

Figure 6 - Schematic illustration of the coupled-flux model for nucleation, showing the interfacial and diffusive rates.

C. AlYFeV – new glasses with large supercooled regions

We found that addition of V to Al-Y-Fe alloys produced glasses having wide supercooled regions, $\Delta T_x = T_x - T_g$ (fig. 6). The width of the supercooled region ΔT_x has been previously associated with glass formability and the stability of the undercooled liquid under "warm" processing treatments such as warm consolidation and injection molding [36, 37, 42, 46, 47]. The ΔT_x values of 80 K reported in Table 1 are the largest known for Al-rich glasses, exceeding the prior record value by 50 K. The V-containing glasses also have high crystallization temperatures T_x, indicative of stable glasses, in comparison to other Al-rich glasses (Table 1).

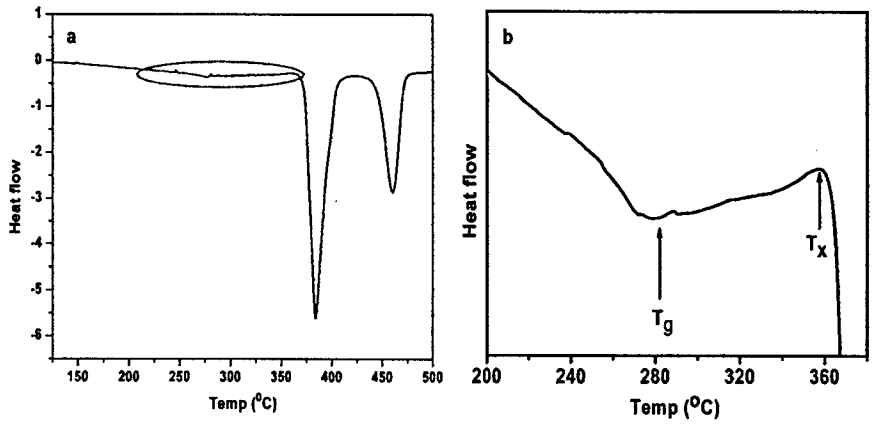

Figure 7 – Non-isothermal DSC data for $Al_{85.35}Y_8Fe_6V_{0.65}$. (a) Full scan; the oval marks the region expanded in b. (b) Expanded region showing the glass-transition temperature T_g, the crystallization temperature T_x, and the wide supercooled region ΔT_x.

The estimated values of the reduced-glass temperatures T_{rg} and γ parameters for the microalloyed Al-rich glasses prepared here (Table 1) are promising indicators that their compositions are near to bulk-glass-forming compositions. The γ parameter (defined in Table 1) was recently introduced [54] as a more-reliable predictor of glass-forming ability (GFA) than the commonly used T_{rg} parameter. Values of $\gamma > 0.40$ and $T_{rg} > 0.6$ are associated with bulk glass formation. The estimated values for the microalloyed V-containing Al-rich glasses in Table 1 at ~0.35 and ~0.48, respectively, are clearly approaching these threshold values. According to Lu and Liu [54], a metallic-glass γ value of 0.35 corresponds to an estimated critical cooling rate of 8.2×10^3 K/s, which is up to two orders of magnitude lower than those of other Al-rich glasses (Table 1). If the γ value could be improved to 0.40, then the estimated critical cooling rate would be 24 K/s. The high measured T_x and ΔT_x values, and the promising estimates of the T_{rg} and γ values suggest that our microalloyed Al-rich glasses are close to bulk-glass-forming compositions. Therefore, further investigations of microaddition and alloy stoichiometries could produce bulk-glass formers in these Al-rich alloy systems at cooling rates in the range of 1-100 K/s, which would have obvious technological impact.

Table 1. Thermal parameters for Al-rich alloy glasses

Glass/Alloy	T_g (°C)	T_x (°C)	$\Delta T_x = T_x - T_g$	T_l (°C)	T_{rg} (T_g/T_l)*	$\gamma = T_x/(T_g + T_l)$*	Ref.
$Al_{84}Ni_{10}Ce_6$	273	286	13	900†	~0.47	~0.33	[4]
$Al_{88}Ni_4Sm_8$	~220	241	21	900†	~0.42	~0.31	[55]
$Al_{88}Y_7Fe_5$	258	280	22	900†	~0.45	~0.32	[43]
$Al_{85}Y_8Ni_5Co_2$	267	297	30	900†	~0.46	~0.33	[47]
$Al_{85}Gd_8Ni_5Co_2$	281	302	21	900†	~0.47	~0.33	[56]
$Al_{85}Dy_8Ni_5Co_2$	277	303	26	900†	~0.47	~0.33	[56]
$Al_{85}Er_8Ni_5Co_2$	274	305	31	900†	~0.47	~0.34	[56]
$Al_{85}Ni_{10}Ce_5$	246	264	18	900†	~0.44	~0.32	[57]
$Al_{85.35}Y_8Fe_6V_{0.65}$	285	**365**	**80**	900†	~0.48	~0.35	‡
$Al_{85}Y_8Fe_6V_{0.65}O_{0.35}$	287	**367**	**80**	900†	~0.48	~0.35	‡
$Al_{87.5}Y_7Fe_5Ti_{0.5}$	275	310	35	900†	~0.47	~0.33	[58]
$Al_{87}Y_7Fe_5Ti_1$	270	340	70	900†	~0.46	~0.34	[58]
$Al_{86}Y_7Fe_5Ti_2$	280	350	70	900†	~0.47	~0.35	[58]
$Al_{87.5}Y_7Fe_5Zr_{0.5}$	275	315	40	900†	~0.47	~0.33	‡
$Al_{87}Y_7Fe_5Zr_1$	295	345	50	900†	~0.48	~0.35	‡
$Al_{86}Y_7Fe_5Zr_2$	310	370	60	900†	~0.50	~0.35	‡
$Al_{87.5}Y_7Fe_5V_{0.5}$	280	340	60	900†	~0.47	~0.34	‡
$Al_{87}Y_7Fe_5V_1$	275	340	65	900†	~0.47	~0.34	‡
$Al_{86}Y_7Fe_5V_2$	280	**360**	**80**	900†	~0.47	~0.35	‡

*The reduced glass-transition temperature T_{rg} and the glass-forming-ability (GFA) parameter γ [54] were calculated using the absolute temperature scale (K).
†Not yet measured; estimated from the relevant binary phase diagrams
‡A. Mukhopadhyay, L.Q. Xing, W.E. Buhro, K.F. Kelton; unpublished.

D. Heterogeneous nucleation on TiB_2

The effectiveness of TiB_2 particles in promoting nucleation in an Al-based metallic glass with a high homogeneous nucleation rate was investigated using the $Al_{87.5}Y_7Fe_5Ti_{0.5}$ glass. Commercially available TiB_2 particles (~ 1-2 μm in diameter) were introduced into the melt during rf-melting in a graphite crucible under an Ar atmosphere. Amorphous ribbons were obtained by rapidly quenching the liquid onto a copper wheel rotating with a surface velocity of ≈ 50 m/s.

Sharp TiB_2 peaks were observed in x-ray diffraction patterns of as-quenched ribbons, and embedded TiB_2 particles in an amorphous matrix were evident in TEM studies. The α-Al crystallization onset temperature decreased with an increasing concentration of TiB_2 and the time-lag for the onset of isothermal crystallization also decreased with increasing TiB_2 concentration. These observations are consistent with a high heterogeneous nucleation rate on the TiB_2 particles. TEM studies of a glass that was annealed for 30 min below the onset of the first peak (280 °C) confirmed this, showing α-Al crystallites on the (011) faces of the TiB_2 particles (fig. 8.a). The α-Al density on the particle is much greater than that in the surrounding amorphous material, indicating that even in this glass, with a high homogeneous nucleation rate (≈ 10^{21}-10^{22} /m^3s), the TiB_2 particles promote heterogeneous nucleation at an even higher rate, ≈ 10^{24}/m^3s normalized to the surface area (fig. 8.b and 8.c). The lower crystal density by homogeneous nucleation is evident in the region near the TiB_2 particle.

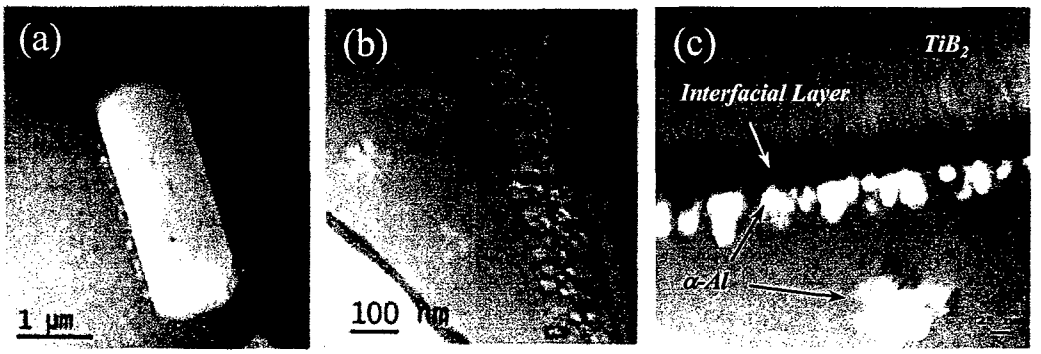

Figure 8 – (a) TEM micrograph of a glass sample containing TiB_2 (after annealing at 280°C for 30 min), showing preferential nucleation of α-Al on the 001 faces of the TiB_2; (b) magnification of the region near the TiB_2 particle, demonstrating a higher density of α-Al on the TiB_2 than in the surrounding amorphous phase; (c) the interfacial reaction layer.

A clearly defined reaction layer, likely Al_3Ti, is observed in figure 8.c. While similar to that observed in heterogeneous nucleation studies in $Al_{85}Y_8Ni_5Co_2$ glasses [59], which have a lower homogeneous nucleation rate than those studied here, it is much thicker (of order 25 μm compared with 3 μm in the $Al_{85}Y_8Ni_5Co_2$ glasses). Further, the α-Al grains appear to be growing into the layer, unlike observations for the $Al_{85}Y_8Ni_5Co_2$ glasses.

These data indicate that the TiB_2 particles are extremely effective nucleating agents. Significant grain refinement would result if nanoparticles of TiB_2 could be uniformly dispersed in the glass.

V. Conclusions

The research supported by AFOSR Grant F49620-01-1-0355 has produced discoveries that directly address many of the questions raised in Section I of this report and suggest future studies that are needed. The key research results are :

- The discovery that a rapidly quenched Al-Y-Fe alloy that has been widely believed to be a glass may be, in fact, a nanostructured composite;

- A demonstration that oxygen contamination dramatically affects glass formation, but does not strongly influence primary crystallization to α-Al;

- The first observation of a dramatic influence of microalloying on glass formation and stability in Al-based glasses, showing that rapidly quenched Al-Y-Fe alloys are true glasses with improved stability against crystallization with the incorporation of small amounts of Ti, Zr, or V (on the level of 0.5 – 1.0 at.%).

- The discovery of a new Al-Y-Fe glass with the largest supercooled region of any Al-based glass ($T_x - T_g$, where T_g is the glass-transition temperature and T_x is the crystallization temperature measured in nonisothermal DSC).

- A demonstration of the catalytic potency of TiB_2 particles as heterogeneous nucleating agents for α-Al in these alloys. Based on the grain density of α-Al on micron-sized TiB_2, if nano-particles of TiB_2 were dispersed uniformly in the glass, an α-Al nanocrystal density of $10^{24}/m^3$ could be achieved, which is 3 orders of magnitude larger than the already enormous grain density from the as-quenched glass containing no inoculants.

These results demonstrate the feasibility of using microalloying and seeding to improve glass formation and nano-structure formation by devitrication of metallic glasses. They have demonstrated that some materials thought to be amorphous may not be, hindering our planned studies of diffusion-limited nucleation and its role in glass formation and stability. However, we have now developed alloys that under carefully controlled processing conditions can be made glassy and we have constructed the theoretical tools that put us in a unique position to make these quantitative nucleation studies.

VI. Questions and Recommendations

In addition to providing these answers, the research has raised several new questions:

- What is the mechanism by which small concentrations of Ti, Zr, and V alter glass crystallization?

- Can further stoichiometric and microaddition modifications produce Al-rich glasses at conventional, slow cooling rates in the range of 1 – 20 K/s?

- Can the FTEM studies of glasses prepared with different composition and under different processing conditions provide insight into glass structure and the role of this microalloying?

- Clearly it is possible to increase the nucleation rate, and hence produce grain refinement, in glasses that already have extremely high homogeneous nucleation rates. Are other MB_2 particles other than TiB_2 perhaps even more effective catalysts?

Several studies were recommended by us to investigate these issues. The recommendations funded under our current AFOSR contract (AFOSR FA9550-05-1-0110) are:

- Structural studies of the Al-TM-RE glasses should be made as a function of microalloying with fluctuation TEM (FTEM), high-angle x-ray diffraction and EXAFS measurements.

- The results of FTEM structural studies should be correlated with isothermal DSC signatures of grain growth and electrical resistivity measurements in other Al-based glasses, as well as computer modeling, to firmly establish the interpretation of the DSC data.

- The particle size densities as a function of annealing time and temperature for as-quenched $Al_{87.5}Y_7Fe_5Ti_{0.5}$ and $Al_{85.35}Y_8Fe_6V_{0.65}$ glasses should be measured and those measurements compared with predictions from the coupled-flux model to make a quantitative check of that kinetic model.

- Additional alloy compositions and microadditive identities should be investigated with the goal of producing bulk-glass-forming Al-rich alloys.

A recommendation that could not be supported due to lack of funds was

- Develop methods for dispersing metal diboride nanoparticles (MB_2) particles in Al-TM-RE-based glasses to evaluate their efficiency in catalyzing nucleation and promoting nanostructure grain refinement. TEM investigations of the interface between the MB_2 particles and the nucleating phases will be made to determine

the mechanism of heterogeneous nucleation and to evaluate models, such as the adsorption model proposed by Cantor *et al.*[60].

The work discussed in this final report and that ongoing under current AFOSR support will significantly improve the understanding of homogenous nucleation mechanisms for production of nanocrystalline composites from metallic glasses. It will lead to a better understanding of microalloying and its role on glass formation. The insight gained from these investigations is a foundation for the development of improved processing strategies that can be used to optimize microstructural design. The information gained from the microalloying studies is also relevant to the fundamental structural studies of glasses being conducted by Dan Miracle at Wright Patterson Air Force Base.

VII. Products and Support

This contract has supported the cost of personnel, publications and conference presentations

A. Publications and Conference Presentations

Publications of research citing partial supported from this contract:

1. K. F. Kelton, T. K. Croat, A. K. Gangopadhyay, L.-Q. Xing, A. L. Greer, M. Weyland, X. Li, K. Rajan, "Mechanisms for nanocrystal formation in metallic glasses," J. Non-Cryst. Solids 2003. **317**: p. 71-77.
2. K. F. Kelton, "Nucleation in glasses and liquids and nanostructure formation," Phys. Chem. Glasses 2004. **45**: p.1-7.
3. L.Q. Xing, A. Mukhopadhyay, W. E. Buhro, and K. F. Kelton, "Improved AlYFe Glass Formation by Microalloying with Ti," Phil. Mag. Lett. 2005. **84**: p.293-302.
4. K. F. Kelton, "Amorphous Metal Formation and Crystallization – Coupled Processes in Crystal Nucleation," J. Metastable and Nanocrystalline Materials 2005. **24-25**: p. 25-30.

Conference presentations of the work citing partial support from this contract:

1. K. F. Kelton and W. E. Buhro, "Studies of Heterogeneous and Diffusion-Influenced Nucleation for Improved Processing of Nanostructural Materials," 2001 Contractors Meeting in Metallic and Ceramic Materials Programs, Snowbird, UT, 19-21 August, 2001.
2. K. F. Kelton, T. K. Croat, A. K. Gangopadhyay, L.-Q. Xing, A. L. Greer, M. Weyland, X. Li, K. Rajan, "Mechanisms for nanocrystal formation in metallic glasses," Advances in Metallic Glasses Symposium of the 131st annual meeting of the TMS, Seattle, WA, 17-21 February 2002.
3. K. F. Kelton, L. Q. Xing and A. K. Gangopadhyay, "Nucleation in Al-RE-TM Metallic Glasses," American Physical Society, 18-22 March, 2002.
4. W. E. Buhro, "Stabilization of Al-Y-Fe Metallic Glasses with Ti," AFOSR Joint 2002 Contractors Meeting in Metallic and Ceramic Materials, Bar Harbor, ME, 12-14 August 2002.
5. L.Q. Xing, A. Mukhopadhyay, W. E. Buhro, K. F. Kelton, "Crystallization of Al-Y-Fe Alloy and the Influence of Small Amount of Ti," Mat. Res. Soc., December 2002.
6. K. F. Kelton, "Nucleation in glasses and liquids and nanostructure formation," K. F. Kelton, Seventh Int. Symp. on Crystallisation in Glasses and Liquids, University of Sheffield, UK, 6-9 July 2003 (Invited Lecture).
7. K. F. Kelton, "Studies of Heterogeneous and Diffusion-Influenced Nucleation for Improved Processing of Nanostructural Materials," AFOSR Joint 2003 Contractors Meeting in Metallic and Ceramic Materials, Boulder, CO, 4-5 August, 2003.

8. K. F. Kelton, "Diffusion Influenced Nucleation – Theory and Case Studies," Precipitation Workshop, Autrans, France, 6-9 October, 2003 (Invited Lecture).
9. W. E. Buhro, 2004 AFOSR Contractors Meeting in Metallic and Ceramic Materials, Wintergreen, VA, 16-18 August 2004, "Nucleation in Aluminum-Based Glasses."
10. K. F. Kelton, Amorphous Metal Formation and Crystallization – Coupled Processes in Crystal Nucleation," 11th International Symposium on Metastable, Mechanically Alloyed and Nanocrystalline Materials (ISMANAM-2004), Sendai, Japan, 22-26 August, 2004 (Plenary Lecture).
11. A. Mukhopadhyay, W. E. Buhro, L. Q. Xing, K. F. Kelton, "Aluminum-Rich Metallic Glasses: Development and Significance," 36th Great Lakes Regional Meeting of the American Chemical Society, Peoria, IL, October 17-20 (2004).

B. Personnel

This contract provided partial summer support for the PI and Co-PI (~ 1 month per year) and two post-doctoral researchers, all located at Washington University, St. Louis, MO.

1. K. F. Kelton, PI, Department of Physics.
2. W. E. Buhro, Co-PI, Department of Chemistry.
3. L. Q. Xing, Post-Doctoral Scientist (1/2 yearly salary).
4. A. Mukhopadhyay, Post-Doctoral Scientist (1/2 yearly salary).

5. References

1. Inoue, A., K. Ohtera, A.P. Tasi, and T. Masumoto, Jpn. J. Appl. Phys., 1988. **27**: p. L280.
2. Inoue, A., K. Ohtera, K. Kita, and T. Masumoto, Jpn. J. Appl. Phys., 1988. **27**: p. L736.
3. He, Y., S.J. Poon, and G.J. Shiflet, Sci., 1988. **241**: p. 1640-42.
4. Inoue, A., Prog. Mater. Sci., 1998. **43**: p. 365-520.
5. Greer, A.L., Nanostructured Mater., 1998. **50**: p. 143-62.
6. Greer, A.L., Mat. Sci. and Eng., 2001. **A304-306**: p. 68-72.
7. Wilde, G., H. Sieber, and J.H. Perepezko, Scripta Mater., 1999. **40**: p. 779-83.
8. Allen, D.R., J.C. Foley, and J.H. Perepezko, Acta Mater., 1998. **46**: p. 431-440.
9. Kelton, K.F., Phil. Mag. Lett., 1998. **77**(6): p. 337.
10. Calin, M. and U. Koester, Mater. Sci. Forum, 1998. **269-272**: p. 749.
11. Kelton, K.F., T.K. Croat, A.K. Gangopadhyay, L.Q. Xing, A.L. Greer, M. Weyland, X. Li, and K. Rajan, J. Non-Cryst. Solids, 2003. **317**(1-2): p. 71-77.
12. Saida, J., J. of Appl. Phys., 2000. **88**(10): p. 6081 EP -.
13. Mattern, N., U. Kühn, H. Hermann, H. Ehrenberg, J. Neuefeind, and J. Eckert, Acta Mater., 2002. **50**: p. 305-314.
14. Xing, L.Q., Y.T. Shen, and K.F. Kelton, Appl. Phys. Lett., 2002. **81**: p. 3371-3373.
15. Das, S.K., J.H. Perepezko, R.I. Wu, and G. Wilde, Mat. Sci. and Eng. A, 2001. **304-306**: p. 159-165.
16. Yoshizawa, Y. and K. Yamauchi, Mater. Trans. JIM, 1990. **31**(4): p. 307-14.
17. Busch, R., S. Schneider, A. Peker, and W.L. Johnson, Appl. Phys. Lett., 1995. **67**: p. 1544.
18. Cini, E., B. Vinet, and P.J. Desre, Phil. Mag. A, 2000. **80**: p. 955-966.
19. Desre, P.J., E. Cini, and B. Vinet, J. Non-Cryst. Solids, 2001. **288**: p. 210-217.
20. Gerold, V. and G. Kostorz, J. Appl. Crystallogr., 1978. **11**: p. 376.
21. Zanotto, E.D., A.F. Craievich, and P.F. James, J. de Physique Coll. 1982. **43**: p.107.
22. Bras, S., A. Craievich, J.M. Sanchez, C. Williams, and E.D. Zanotto, Nuc. Instr. and Meth. in Phys. Res, 1983. **208**: p489.
23. Zanotto, E.D., P.F. James, and A.F. Craievich, J. Mater. Sci., 1986. **21**(9): p. 3050.
24. Hono, K. and K.-I. Hirano, Phase Transitions, 1987. **10**: p. 223.
25. Schneider, S., Thiyagarajan, P., Geyer, U., Johnson, W.L., Physica B., 1997. **241-243**: p. 918.
26. Takei, T., Y. Kameshima, A. Yasumori, K. Okada, N. Kumada, and N. Kinomura, J. Non-Cryst. Solids, 2001. **282**: p. 265-277.
27. Hono, K. and T. Sakurai, App. Surface Sci., 1995. **87-88**: p. 166.
28. Busch, R., S. Schneider, A. Peker, and W.L. Johnson, Appl. Phys. Lett., 1995. **67**(11): p. 1544.
29. Miller, M.K., R.B. Schwarz, and Yi He, Bulk Metallic Glasses. Symposium. 1999: Mater. Res. Soc.

30. Read, H.G., K. Hono, A.P. Tsai, and A. Inoue. Mat. Sci and Eng., 1997. **A226-228** : p. 453.
31. Inoue, S., A. Makishima, H. Inoue, K. Soga, T. Konishi, and T. Asano, J. Non-Cryst. Solids, 1999. **247**: p. 1-8.
32. Hono, K., K. Hiraga, Q. Wang, A. Inoue, and T. Sakurai, Acta Metall. et Mater., 1992. **40**(9): p. 2137.
33. Perepezko, J.H. and W.S. Tong, Phil. Trans. Royal Soc., 2002. **361**(1804): p. 447 - 461.
34. Perepezko, J.H. and R.J. Herbert, J. of Metals, 2002. **54**(3): p. 34-39.
35. Kelton, K.F. and A.L. Greer, J. Non-Cryst. Solids, 1986. **79**(295-309).
36. Choi-Yim, H., R. Busch, and W.L. Johnson, J. Appl. Phys., 1998. **83**: p. 7993.
37. Lu, Z.P., C.T. Liu, and W.D. Porter, Appl. Phys. Lett., 2003. **83**: p. 2581.
38. Yim, H.C., R. Busch, and W.L. Johnson, J. Appl. Phys., 1998. **83**: p. 7993.
39. Zhang, Y., M.X. Pan, D.Q. Zhao, R.J. Wang, and W.H. Wang, Mat. Trans. JIM, 2000. **41**: p. 1410.
40. Kundig, A.A., D. Lepori, A.J. Perry, S. Rossmann, A. Blatter, A. Dommann, and P.J. Uggowitzer, Mat. Trans. JIM, 2002. **43**: p. 3206.
41. Liu, C.T., M.F. Chisholm, and M.K. Miller, Intermetallics, 2002. **10**: p. 1105.
42. Wang, W.H., Q. Wei, and H.Y. Bai, Appl. Phys. Lett., 1997. **71**: p. 58.
43. Foley, J.C. and J.H. Perepezko, J. Non-Cryst. Solids, 1996. **205-207**: p. 559-562.
44. Chen, L.C. and F. Spaepen, J. Appl. Phys., 1991. **69**(2): p. 679-688.
45. Kelton, K.F. and J.C. Holzer, Rev. Sci. Instrum., 1988. **59**: p. 347.
46. Inoue, A., T. Zhang, and T. Masumoto, Mat. Sci. and Eng., 1991. **A134**: p. 1125.
47. Louzguine, D.L. and A. Inoue, Mater. Lett., 2002. **54**: p. 75.
48. K. F. Kelton, *Solid State Physics*, (H. Ehrenreich and D. Turnbull, eds.), Academic Press, 1991. **45**: p. 75-178.
49. K. F. Kelton and A. L. Greer, J. Non-Cryst. Solids, 1986. **79**: p. 295-309.
50. Kelton, K.F., Acta Mater., 2000. **48**(8): p. 1967.
51. Kelton, K.F. J. Non-Cryst. Solids, 2000. **274**: p. 147-154.
52. Russel, K. C., Acta Metall., 1968. **16**; p. 761.
53. Kelton, K. F., Phil. Trans. R. Soc. Lond. A, 2003. **361**: p.429-445.
54. Lu, Z.P. and C.T. Liu, Phys. Rev. Lett., 2003. **91**: p. 115505 1-4.
55. Gich, M., T. Gloriant, A.L. Surinach, A.L. Greer, and M.D. Baro, J. Non-Cryst. Solids, 2001. **289**: p. 214-220.
56. Louzguine, D.L. and A. Inoue, Appl. Phys. Lett., 2001. **79**: p. 3410-12.
57. Si, P., X. Bian, J. Zhang, H. Li, M. Sun, and J. Zhao, J. Phys.: Condens. Matter., 2003. **15**: p. 5409-15.
58. Xing, L.Q. Xing, Mukhopadhyay, A., Buhro, W. E., and Kelton, K. F., ,Phil. Mag. Lett. 2005. **84**: p.293-302.
59. Schumacher, P., Greer, A. L., Mat. Sci. Eng., 1994, A181-182: p. 1335.
60. Kim, W.T. and B. Cantor, Acta Metall. Mater., 1994. **42**: p. 3115.